Macromolecules

pubs.acs.org/Macromolecules Article

Pivotal Roles of Triple Screening-Topological, Electrostatic, and Hydrodynamic-On Dynamics in Semidilute Polyelectrolyte Solutions

Rajeev Kumar,* Ali H. Slim, Antonio Faraone, Jan-Michael Y. Carrillo, Ryan Poling-Skutvik, Murugappan Muthukumar, Amanda B. Marciel, and Jacinta C. Conrad*

Cite This: *Macromolecules* 2024, 57, 2888−2896 Read Online

ACCESS | Metrics & More | Article Recommendations | Supporting Information

ABSTRACT: For semidilute polyelectrolyte solutions, it is generally assumed that topological, electrostatic, and hydrodynamic interactions are screened (called triple screening). Despite a large body of research focused on polyelectrolyte solutions, the concept of triple screening has never been rigorously verified. In this work, we test the concept by probing concentration fluctuations in aqueous solutions containing a well-studied polyelectrolyte, sodium poly(styrenesulfonate) (NaPSS) with neutron scattering, theory, and molecular dynamics simulations. Neutron spin−echo (NSE) and small-angle neutron scattering (SANS) data from semidilute solutions of NaPSS are presented at different polymer and salt (NaCl) concentrations. A combined theory for structure (*J. Chem. Phys.* 105, 5183 (1996)) and dynamics (*J. Chem. Phys.* 107, 2619 (1997)), which captures effects of hydrodynamic, topological, and electrostatic screening, is used to interpret the experimental results. The theory quantitatively predicts the decay rate obtained from the NSE measurements while capturing the shape and concentration dependencies of the polyelectrolyte peak observed in the SANS spectra. Detailed comparisons of the theory and the experiments reveal that the wavevector-dependent decay rate of concentration fluctuations in semidilute solutions of polyelectrolytes is dictated by the screening of hydrodynamic, topological, and electrostatic interactions. This conclusion is corroborated by coarse-grained molecular dynamics simulations, executed without any hydrodynamic interactions, which fail to capture the correct wavevector dependence of the decay rate. These results highlight that the theories based on the concept of triple screening provide a quantitative framework for predicting a relation between the structure and dynamics of polyelectrolyte solutions.

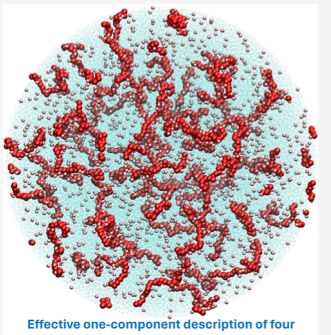

1. INTRODUCTION

A fundamental understanding of the ubiquitous processes of assembly and dynamics of charged macromolecules,[1−10] such as DNA, intrinsically disordered proteins, and synthetic polyelectrolytes and polyampholytes in aqueous solutions, remains a grand challenge in soft and living matter. The origin of this challenge[9,10] lies in the interdependent confluence of three long-ranged forces arising from (1) topological correlations due to chain connectivity, (2) electrostatic interactions among all charged species, and (3) hydrodynamic interactions pervading throughout the system. This confluence is orchestrated by the various molecular and atomic attributes of all constituents in the system, such as the composition of macromolecules, chemical nature, charge sequence, and length of the various macromolecules, concentration of added low molar mass salt, pH, and temperature.

Even in the simplest case of uniformly charged polyelectrolytes dispersed in aqueous solutions containing monovalent electrolyte ions, the phenomenology of assembly and dynamics exhibits a rich and counterintuitive physics. For example, even though all of the chains are similarly charged, they can interpenetrate into each other and exhibit structure [as a "polyelectrolyte peak" in scattering experiments,[11] such as small angle neutron scattering (SANS)] at intermediate length scales between that of the size of isolated chains and size of the monomers composing the macromolecules. Another example is that the diffusion coefficient measured for uniformly charged macromolecules under salt-free conditions can exhibit distinct regimes of dynamics delineated by the ordinary−extraordinary transition, which is commonly attributed to the collective behavior of the chains in their electrostatic environment emanating from their counterions.[9,12] Furthermore, similarly charged macromolecules can, instead of repelling, aggregate into large scale structures in salt-free conditions, as exhibited by the simultaneous occurrence of the enhanced scattering intensity corresponding to large length scales,[9,10,13] and the slow mode in dynamic light scattering (DLS) studies.[11] Until recently,[14] however, the structure and dynamics in these systems were mainly investigated separately.

To explain these surprising observations, a number of theories[15−24] for concentration fluctuations in polyelectrolyte

Received: December 13, 2023
Revised: February 16, 2024
Accepted: February 28, 2024
Published: March 15, 2024

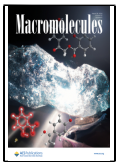

https://doi.org/10.1021/acs.macromol.3c02564
Macromolecules 2024, 57, 2888−2896

solutions have been reported in the literature. These theories invoke different approximations such as weak inhomogeneity [known as the random phase approximation (RPA)] and screened hydrodynamic interactions to simplify the description of multicomponent polyelectrolyte solutions containing polymer chains, counterions, co-ions, and solvent. Notably, the results of coarse-grained molecular dynamics simulations executed without any hydrodynamics[25−32] are in disagreement with many of the predictions made by these theories. Some of these theories[18,19,23] consider the effects of hydrodynamic interactions and screening from multiple chains, counterions, and co-ions, but treat electrostatic screening from the chains and ions (i.e., counterions and co-ions) either by invoking RPA or by a self-consistent variational approach. In addition, scaling arguments[3,7,33] have been developed to interpret experimental results for the dependencies of correlation length ξ and viscosity of polyelectrolyte solutions on molecular weight, salt, and polymer concentrations. For the dynamics in polyelectrolyte solutions, these scaling arguments[33] are based on the Rouse model applied to a chain of correlation blobs, which ignores hydrodynamic effects by assuming that they are screened on a length scale larger than ξ. In a recent development, scaling arguments for the dynamics in salt-free semidilute unentangled polyelectrolyte solutions are used to determine the molecular weight of polyelectrolytes.[34] Despite these developments, the central assumption that hydrodynamic interactions are screened in semidilute polyelectrolyte solutions remains unverified. Thus, it is of utmost importance to establish a clear and quantitative connection between the structure and dynamics at the length scale of polyelectrolyte chains. Such an understanding is necessary to make progress in the development of new polymer electrolytes[35−37] and polyelectrolyte membranes.[38]

Here, we compare SANS and neutron spin echo (NSE) measurements[14] to theoretical predictions[22,23] that account for electrostatic, hydrodynamic, and structural screening effects. When the effects of electrostatic and structural screening are included in theory, we obtain only qualitative agreement between the experiment and predictions. Inclusion of hydrodynamic interactions is required for a quantitative agreement. By analyzing the experimental data with the use of Muthukumar's theory of structure[22] and dynamics[23] of polyelectrolytes with closed-form formulas, we identify the fundamental principles behind the structure-dynamics duality in solutions containing charged macromolecules. The combination of experiment and theory provides a conceptual platform to quantitatively interpret structural and dynamic data on charged macromolecules.

2. MATERIALS AND METHODS

2.1. Sample Preparation. Glass vials were soaked overnight to ensure near salt-free conditions in a base bath solution of 6.5% weight fraction potassium hydroxide in isopropanol. Residual salt was removed by rinsing vials ten times using Millipore water. The vials were then dried in an oven for 2 h at 105 °C. Sodium poly(styrenesulfonate) (NaPSS) with a weight-averaged molecular weight Mw = 68,300 Da (Scientific Polymer Products) was dissolved in deuterium oxide (Sigma-Aldrich) or Millipore water at three different ionic strengths. The ionic strength of deuterium oxide and deionized water was assumed to be 10^{-6} mol L^{-1} (hereafter M). The ionic strength of the other two sets of solutions was adjusted by adding sodium chloride to achieve (10^{-2} and 10^{-1}) M. We determined intrinsic viscosity η by fitting the data to the two term virial expansion of viscosity $\eta = \eta_0(1 + c/c^*)$, where η_0 is the solvent viscosity, and c^* is the overlap concentration, estimated to be (12.3, 15.7, and 31.9) g L^{-1} at (10^{-6}, 10^{-2}, 10^{-1}) M ionic strength, respectively. The radius of gyration was estimated via $R_{g,0} = M_w/(4/3\pi c^* N_{av})^{1/3}$. The estimated $R_{g,0}$ values were (13, 12, and 9.5) nm at (10^{-6}, 10^{-2}, and 10^{-1}) M, respectively.

Certain trade names and company products are identified in order to adequately specify the experimental procedure. In no case does such identification imply recommendation or endorsement by the National Institute of Standards and Technology, nor does it imply that the products are necessarily the best for the purpose.

2.2. Bulk Rheology. Polymer solutions in deionized water were loaded into a single-gap Couette cell with a cup diameter of 15 mm, a bob diameter of 14 mm, and an effective bob length of 42 mm. Steady-shear measurements of the rate-dependent viscosity were performed on a Discovery Hybrid Rheometer (TA Instrument, HR-2). Instrument torque and inertia were calibrated and samples were presheared at 1000 s^{-1} for 1 min prior to measurements. For measurements, solutions were presheared for 1 min at the measurement shear rate to reach equilibrium, after which the average viscosity across 1 min was determined. These results are shown in Figure S1.

2.3. Neutron Scattering. We prepared three sets of NaPSS solutions in deuterium oxide at three different ionic strengths. Deuterium oxide was used as the solvent to minimize the incoherent scattering contribution to total scattering. The polymer concentrations were chosen to obtain similar chain structural properties (i.e., correlation length) for samples at different ionic strengths according to de Gennes' scaling predictions. We estimated the scattering length densities in 10^{-6} $Å^{-2}$ to be 1.140 for NaPSS and 6.393 for deuterium oxide, which provided sufficient contrast to isolate the scattering signal from polyelectrolyte chains. Samples were loaded into 4 mm thick titanium demountable cells to ensure a transmission of 60−70%. We collected small-angle neutron scattering (SANS) and NSE on the NGB-30 and NSE beamlines, respectively, at the Center for Neutron Research, National Institute of Standards and Technology (NIST). SANS was performed at all available configurations including lenses and sample to detector distances (1, 4, and 13 m) to achieve a wavevector range of 0.001−0.5 $Å^{-1}$, corresponding to length scales of 1.3−630 nm. The raw SANS data was reduced to an absolute intensity by correcting for the blocked beam scattering, empty cell scattering, and detector sensitivity using IgorPro. NSE was collected at two incident wavelengths (6 and 8 Å) to acquire data across a wavevector range of 0.05−0.26 $Å^{-1}$, corresponding to length scales of 2.4−12.6 nm. The data were scaled to account for the solvent dynamics and instrument resolution by measuring the echoes of pure deuterium oxide and a charcoal standard, respectively. The DAVE software package[39] was used to reduce NSE data. All measurements were performed at room temperature.

2.4. Double Screening Theory for Structure in Polyelectrolyte Solutions.[22] In very dilute solutions, uniformly charged polyelectrolyte chains stay away from each other due to their electrostatic repulsion, with an average distance between a pair of chains given as $c^{-1/3}$, where c is the polymer concentration, based on the geometrical packing consideration. As c is increased, the gain in conformational entropy by the chains upon their interpenetration overwhelms the interchain electrostatic repulsion. As a result, the chains do indeed interpenetrate for c above overlap concentration c^*. A direct consequence of chain interpenetration is that the original electrostatic interaction between two charged monomers of a labeled chain is now screened by the intervening chains. The extent of screening, called topological screening (also known as the Edwards screening in uncharged polymer systems), is characterized by a topological screening length ξ, which depends not only on the concentration of intervening chains but also on the topological correlation of the intervening chains due to their chain connectivity.

Since the ionized polyelectrolyte chains cannot exist alone without their dissociated counterions, the aqueous medium containing the chains is an electrolyte solution consisting of the counterions as well as the added salt ions. It is well-known that the Coulombic

https://doi.org/10.1021/acs.macromol.3c02564
Macromolecules 2024, 57, 2888−2896

electrostatic interaction between any two charged species in an electrolyte solution is modified into the screened Coulombic interaction with a characteristic screening length (Debye length ξ_D) that is dictated by the ionic strength of the medium. Therefore, any two charged monomers of the polyelectrolyte chains in the neutralizing aqueous background are subjected to this kind of electrostatic screening arising from small dissociated counterions and dispersed salt ions. In reality, both kinds of screening (topological and electrostatic) occur simultaneously and these must be determined self-consistently. Starting from reliable parametrization of chain connectivity and intermonomer short-range van der Waals excluded volume interactions using the Edwards path integral formalism, and incorporation of electrostatic interactions among all charged species in the system, Muthukumar's double screening theory[22,40] treats the self-consistent confluence of topological and electrostatic screenings and presents closed-form analytical formulas for the topological screening length ξ in terms of polyelectrolyte concentration, added salt concentration, and the solvent quality (in terms of short-ranged excluded volume interaction and temperature). Relegating the field-theoretic technical details to the original publications,[22,40] the key conclusions pertinent to scattering experiments are as follows.

(i) The topological screening length ξ is a crossover function of polymer concentration c. In general, in the salt-free limit[40]

$$\xi \sim c^{-\beta} \tag{1}$$

where β changes from 1/3 for very dilute solutions to 1/2 for semidilute solutions. Thus, depending on the polymer concentration, an apparent value of the exponent in the range of 1/3 to 1/2 can emerge.

(ii) The topological screening length ξ is a crossover function of the added salt concentration c_s. For semidilute solutions, in the limit of zero-salt

$$\xi \sim c^{-1/2}, \quad \text{for} \quad c_s \to 0 \tag{2}$$

and in the high salt concentration limit

$$\xi \sim c^{-3/4}, \quad \text{for high} \quad c_s \tag{3}$$

These results are valid in the semidilute conditions where the concentration fluctuations are strong. The result of eq 2 is different from several other theoretical works, suggesting $\xi \sim c^{-1/4}$. It is to be noted that eq 3 is equivalent to the result of uncharged flexible polymer chains in semidilute good solutions. Therefore, by combining eqs 2 and 3, the exponent for the concentration dependence of ξ crosses over from $-1/3$ to $-3/4$ depending on the polymer concentration and salt concentration. In general, the magnitude of this exponent increases as the polymer concentration and salt concentration are increased.

(iii) The predicted scattering intensity $I(q)$, where q is the scattering wave vector in semidilute solutions, is given in the limit of low salt concentration as

$$\frac{I(q)}{I(q \to 0)} = \frac{q^2}{1 + q^4\xi^4} \tag{4}$$

where $\xi \sim c^{-1/2}$ (cf. eq 2). According to eq 4, the scattering intensity exhibits a peak ("polyelectrolyte peak") at the intermediate scattering wave vector $q^* = \xi^{-1} \sim c^{1/2}$. If the polymer concentration is not high enough to be in the fully semidilute regime, the crossover nature of the exponent β given in eq 1 needs to be accounted for in describing the dependence of q^* on c.

(iv) In contrast with the low salt concentration limit, the above formula crosses over in the high salt concentration limit into the familiar Ornstein–Zernike form

$$\frac{I(q)}{I(q \to 0)} = \frac{1}{1 + q^2\xi^2} \tag{5}$$

where $\xi \sim c^{-3/4}$ (cf. eq 3). The "polyelectrolyte peak" is destroyed by the extensive screening of electrostatic interactions in the high salt concentration limit.

2.5. Theory for Dynamics of Polyelectrolyte Solutions.[23]

While the dynamics of the polyelectrolyte chains are driven by the equilibrium structures, which in turn emerge from the coupled double screening of topological and electrostatic correlations, these interactions are mediated by the hydrodynamic interactions among all monomers in the system. This long-ranged hydrodynamic interaction between a pair of monomers is also screened by the interpenetration of chains, just like the electrostatic and topological interactions. Thus, it is necessary to self-consistently treat the triple screening for the three long-ranged interactions. Treating this triple screening, by explicitly considering hydrodynamics in polyelectrolyte solutions in addition to the above-mentioned electrostatic and topological correlations, Muthukumar's theory[23] gives the decay rate $\Gamma(q)$ for the time-dependence of the monomer concentration fluctuations. In particular, the time (t)-dependent equation for the qth Fourier component of monomer density ($c(\mathbf{q}, t)$) can be written as

$$\frac{\partial c(\mathbf{q}, t)}{\partial t} = -\Gamma(\mathbf{q}) c(\mathbf{q}, t) \tag{6}$$

where $\Gamma(\mathbf{q})$ is the wavevector dependent Onsager's coefficient, which can be written as

$$\Gamma(\mathbf{q}) \equiv q^2 D_c(q) = k_B T \int \frac{d^3\mathbf{k}}{(2\pi)^3} \frac{S_{pp}(\mathbf{k}+\mathbf{q})}{S_{pp}(\mathbf{q})} \frac{[q^2 - (\hat{\mathbf{k}}\cdot\mathbf{q})^2]}{[\eta_0 k^2 + \Sigma(\mathbf{k})]} \tag{7}$$

where η_0 is the viscosity of the solvent, and S_{pp} is the equilibrium structure factor, given by (cf. eq 4)

$$S_{pp}(\mathbf{q}) = \frac{1}{c(w + w_c/\kappa^2)} \frac{q^2}{q^4\xi^4 + 1} \tag{8}$$

in the low salt limit. Here, w is the excluded volume parameter characterizing short-ranged monomer–solvent interactions, ξ is the correlation length, and $w_c = z_p^2 e^2/\epsilon k_B T$ so that z_p is the valency of the charge on a polymer segment. κ^{-1} is the Debye screening length involving dissociated ions from the polyelectrolytes and salt ions. Explicitly, $\kappa^2 = e^2(z_c^2\rho_c + \sum_{\gamma=\pm} z_\gamma^2 \rho_\gamma)/\epsilon k_B T$ so that z_c is the valency of the counterions of the charged polymers, $\gamma = \pm$ denotes the ions introduced by the salt, and $\rho_{j=c,+,-}$ represents number densities of ions of type j. e is the charge of an electron, ϵ is the permittivity of the solvent, k_B is the Boltzmann's constant, and T is the temperature. Also, a wavevector-dependent cooperative diffusion constant ($=D_c(q)$) has been defined by the ratio $\Gamma(q)/q^2$.

Note that the denominator of the last term in eq 7 denotes the hydrodynamics of the whole fluid that contains all chains. The factor $\Sigma(\mathbf{k})$ is the result of all contributions from the chains to the net hydrodynamic behavior of the solution. It has been shown[41,42] that $\Sigma(\mathbf{k}) = (\eta - \eta_0)k^2$ in the limit of $k \to 0$, which is of relevance to the scattering experiments, and that $\Sigma(\mathbf{k}) = \eta_0 \xi_h^{-2}$ for $kR_g \gg 1$. Here, η_0 and η are the viscosities of the solvent and the solution, respectively, and ξ_h is the hydrodynamic screening length that is proportional to the static screening length.[23] Therefore, in comparison with data on the decay rate of concentration fluctuations in the small scattering angle limit (as in DLS and NSE), the denominator of the hydrodynamics component in eq 7 is ηk^2, and hence the viscosity of the solution, instead of the viscosity of the solvent, must be used.

In addition to the triple screening used in obtaining the above result, there is the omnipresent coupling of the dynamics of the counterion cloud that hovers around the polyelectrolyte chains. The above result, eq 7, is valid only if the coupling of the chain dynamics with that of the counterion cloud is ignored, which is valid only if the added salt concentration is high. In general, the coupling between the chain dynamics and counterion cloud dynamics must be accounted for because they are not independent, in addition to the collective effects of the triple screening. When this coupling is taken into account, the general result for the decay rate is[23]

https://doi.org/10.1021/acs.macromol.3c02564
Macromolecules 2024, 57, 2888−2896

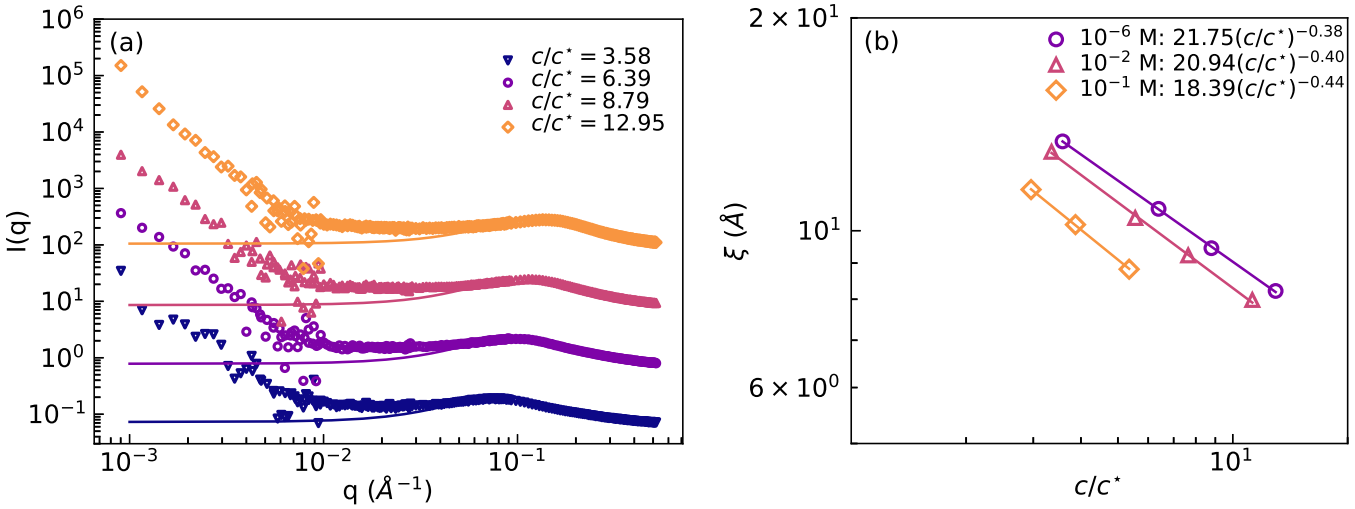

Figure 1. (a) SANS data for salt-free solutions of NaPSS at different polymer concentrations (symbols) and fits of the polyelectrolyte peaks to theoretically predicted functional form ($I(q) \sim q^2/(1 + q^4\xi^4)$) (lines). SANS curves are shifted vertically for clarity. (b) Correlation length ξ, extracted from SANS data over a wavelength range $0.05 \leq q \leq 0.26$ Å^{-1} near the polyelectrolyte peak, as a function of normalized NaPSS concentration c/c^* for three different salt concentrations. Expressions for the fitted lines to the correlation lengths are shown in the legends, which appear as straight lines in the figure plotted on log-scale.

$$\Gamma(q) = D_c(q)\left[1 + \frac{\kappa_1^2 M_1}{D_c(q)[q^2 + \kappa^2]}\right]q^2 \tag{9}$$

Here, κ_1 is the inverse of the Debye length arising solely from the counterions (i.e., without salt ions), and κ is the inverse Debye length arising from both the counterions and salt ions. M_1 is the diffusion coefficient of a segment. In view of the relation $\kappa^2 \sim c_s$ in the denominator of the second term inside the square brackets in eq 9, the second term is negligible for high salt concentrations, and thus the coupling between the counterion cloud dynamics and chain dynamics is broken and D_c is given by eq 7.

Equation 6 leads to a semianalytical expression for the effective monomer−monomer dynamic structure factor

$$\langle c(\mathbf{q}, t)c(\mathbf{q}, 0)\rangle = \exp[-\Gamma(\mathbf{q})t]\langle c(\mathbf{q}, t)c(\mathbf{q}, 0)\rangle_{t\to 0} \tag{10}$$

The theory leads to an effective one-component description of the solutions so that the degrees of freedom of the counterions and solvent are integrated out. This greatly simplifies the mathematical analysis and only the effective monomer−monomer structure factor ($S_{pp}(\mathbf{q})$) appears in eq 7. In the Supporting Information, we show some representative results obtained by evaluating eq 7 numerically.

3. RESULTS

To understand the relationship between structure and dynamics, we collected SANS data on NaPSS solutions at varying polymer and salt (NaCl) concentrations.[14] SANS experimental data for the salt-free NaPSS solutions (Figure 1) confirm that the solutions are in the semidilute regime.[14] For all solutions, the scattering intensity exhibits a local maximum called the "polyelectrolyte peak" at a finite wavevector, q^*, and upturns at lower wavevectors (Figure 1a and Figure S2). The polyelectrolyte peak shifts to higher wavevectors with an increase in polymer concentration c, indicating that the characteristic length scale decreases. The width of the peak reflects changes in the polymer stiffness, which depends on salt and polymer concentrations.[14] We perform SANS measurements on samples with various salt concentrations and extract the correlation length ξ by fitting the peak to the theoretically predicted[22] functional form $I(q) = Aq^2/(1 + q^4\xi^4)$, where A and $\xi = 1/q^*$ are fitting parameters related to contrast factors and the correlation length, respectively. To compare the polymer concentration dependence of ξ for various salt concentrations, we report polymer concentration normalized by the overlap concentration, c^*, where the latter was estimated from the measured viscosity data (Figure S1) to be 12.3, 15.7, and 31.9 g L^{-1} at 10^{-6}, 10^{-2}, and 10^{-1} mol L^{-1} (hereafter, indicated as M) ionic strength, respectively. For a fixed c/c^*, ξ increases as the salt concentration decreases, and electrostatic screening becomes weaker. Furthermore, ξ decreases as a power-law with c/c^*, i.e., $\xi \sim (c/c^*)^{\nu}$, where $0.38 \leq \nu \leq 0.44$ as chains begin to interpenetrate more.

The scaling exponents determined in our SANS experiments as well as others[40,43,44] show that the RPA, which predicts $\xi \sim 1/c^{1/4}$, is not valid in semidilute solutions. This discrepancy likely arises due to the breakdown of weak inhomogeneity and stronger electrostatic correlations in the solutions. In semidilute polyelectrolyte solutions, however, electrostatic correlations couple to the correlations resulting from short-range interactions due to interpenetration of chains (i.e., for $c > c^*$). Thus, we consider the double screening picture,[22] which posits that the interactions between charged monomers on the polyelectrolyte chains are subject to topological screening due to interpenetrating chains and electrostatic screening arising from small dissociated counterions and dispersed salt ions. To test the validity of this picture, we compare the dependence of ξ on polymer and salt concentration to predictions from scaling arguments[33] and those derived from a variational method.[22] Both theories predict that $\xi \sim 1/c^{\nu}$, such that ν changes from 1/3 to 1/2 across the transition from the dilute to the semidilute regime of polyelectrolyte solutions.[7,9,22,33,40] In our study, the exponent $\nu \in [0.38, 0.44]$ (Figure 1b) confirms that the transition from dilute to semidilute regime is gradual, in agreement with previously published studies by several groups and presented as a master curve by Muthukumar.[40] Here, we should point out that it is not possible to collapse the data for different salt concentrations because only limiting laws for the dependence of the correlation length on the salt concentration are available (e.g., see Table 1 in ref 23). Full parametric dependence comes from the solution of an integral equation, which we have not

https://doi.org/10.1021/acs.macromol.3c02564
Macromolecules 2024, 57, 2888−2896

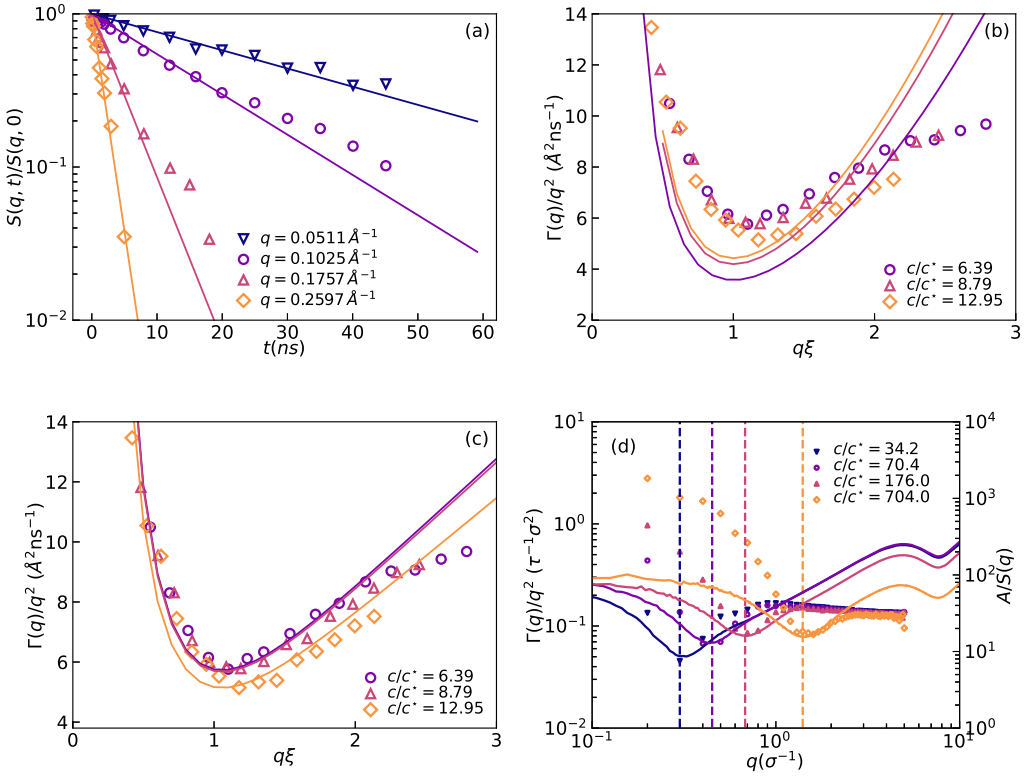

Figure 2. (a) Fits of the NSE data to $\exp[-\Gamma(q)t]$ for salt-free NaPSS solutions ($c/c^* = 6.39$). NSE data was collected for 15 different wavevectors. (b) $\Gamma(q)/q^2$ as a function of q for experimental data for salt-free NaPSS solutions (symbols) and for a theoretical model using $\Gamma(q) = q^2 D_0 k_B T/S_{pp}(q)$, after estimating $S_{pp}(q)$ from the SANS data and taking D_0 as a fit parameter. (c) $\Gamma(q)/q^2$ for salt-free NaPSS solutions along with the fits to eq 11 at three polymer concentrations. Data for the other salt concentrations are provided in Figure S3 in Supporting Information. (d) $\Gamma(q)/q^2$ as a function of q for molecular dynamics simulations without hydrodynamic interactions.

attempted. Nevertheless, the fitting of the polyelectrolyte peak to $I(q) = Aq^2/(1 + q^4\xi^4)$ and the scaling of $\xi \sim (c/c^*)^{\nu}$ confirm the double screening in polyelectrolyte solutions, where polyelectrolyte chains and dissolved ions participate in screening of interactions.

Next, we examined the effects of these screened interactions on the collective dynamics. NSE data were collected[14] at two incident wavelengths (6 and 8 Å) to access a wavevector range of $0.05 \leq q \leq 0.26$ Å^{-1}, corresponding to length scales of approximately 2.4−12.6 nm (Figure 2a). The NSE data were fitted to a single exponential of the form $\exp[-\Gamma(q)t]$ to extract a wavevector dependent decay rate, $\Gamma(q)$, of the collective monomer density-monomer density correlation function. This fitting procedure is motivated by the theoretically predicted exponential functional form,[9,23,40] which is based on an assumption that the time scale for relaxation of counterion and co-ion densities is much lower than the relaxation time of monomer density fluctuations. In ref 14, a stretched exponential functional form was used to fit the same experimental data, and in the short time limit (strictly, in the limit of $t \to 0$), these two functional forms (i.e., a single exponential and the stretched exponential) give similar results for the decay rate.

The decay rate $\Gamma(q)$, which in NSE captures the time-dependence of the monomer concentration fluctuations, increases monotonically with q for the three salt concentrations in the semidilute concentration regime (shown in Figure 2a for salt-free solutions; results for the other solutions are shown in Figure S3 in the Supporting Information). However, $\Gamma(q)/q^2$ exhibits a distinct nonmonotonic behavior with minima around $q\xi \sim 1$ (Figure 2b), indicating that the measured dynamics are nondiffusive. This nonmonotonic behavior is observed for all salt-free solutions as well as for solutions containing 0.01 and 0.1 M NaCl (see Figure S3 in Supporting Information). The close agreement between the minima in Γ/q^2 and the structural peak at $q^* = 1/\xi$ implies that the structural conformations of the polyelectrolyte chains in solution can affect the chain dynamics. Typically,[45−47] structural effects are incorporated into the wavevector dependence of $\Gamma(q)$ through $\Gamma(q) = q^2 k_B T \mu(q)/S_{pp}(q)$, where $S_{pp}(q)$ is a monomer density-monomer density correlation function, $\mu(q)$ is a wavevector dependent mobility, and $k_B T$ is the product of the Boltzmann constant and temperature. As a first attempt to capture the observed nondiffusive relaxations in semidilute polyelectrolyte solutions, we assume that $\mu(q) = D_0$ is independent of q and fit $\Gamma(q)/q^2$ with $k_B T D_0/S_{pp}(q)$. This approach leads to qualitative and quantitative discrepancies (Figure 2b) between the predicted and measured relaxation rates, indicating that the wavevector dependence of $\mu(q)$ arising from hydrodynamic interactions[48] must be taken into account.

For semidilute polyelectrolyte solutions, such an expression for $\Gamma(q)$ was obtained in ref 23 leading to (see Section 2.5 and Figures S4−S10 in the Supporting Information)

$$\Gamma(q) = \frac{k_B T}{\eta}\left[1 + \frac{\kappa_1^2 M_1}{q^2 + \kappa^2}\right]\int_0^\infty \frac{dk'}{(4\pi^2)}\frac{S_{pp}(k')}{S_{pp}(q)}k'^2 \left[\frac{k'^2 + q^2}{2k'q}\ln\left|\frac{k' + q}{k' - q}\right| - 1\right] \quad (11)$$

https://doi.org/10.1021/acs.macromol.3c02564
Macromolecules 2024, 57, 2888−2896

where η is the solution viscosity, and κ^{-1} is the Debye screening length resulting from the presence of counterions and co-ions. This equation captures the collective dynamics of polyelectrolyte chains resulting from the equilibrium solution structure and the coupled double screening of topological and electrostatic correlations mediated by long-range hydrodynamic interactions. Equation 11 was derived by starting from the Langevin equations for motion of Kuhn segments, which involves forces resulting from intrachain and interchain interactions, and thermal forces convoluted with a mobility tensor that captures hydrodynamic effects. The factor of $\kappa_1^2 M_1$ results from an assumption that time scales for relaxation of counterion and co-ion densities are much shorter than relaxation of the monomer density (see the Materials and Methods section for its expression). In general, the relaxation of the counterions and co-ions and that of the monomer concentration are coupled. In fact, this is the essence of the coupling theory developed by one of the authors[10,12,23,49] (e.g., see Sections 7.6.3 and 7.7.4 in ref 10). Briefly, the rate of relaxation of the polymer concentration is coupled to that of the ion cloud around each segment. Thus, there are two relaxation equations, one for the polymer concentration and the other for the ion cloud. An exact solution of the two coupled equations gives two relaxation rates Γ_1 and Γ_2 (as given by eq (7.6.19) in ref 10). One of these rates (Γ_1) is nondiffusive and superfast, and this mode is known as the Debye mode or plasmon mode. The other (Γ_2) is usually labeled as the fast mode and is diffusive (given for example by eq (7.6.23) in ref 10). As shown in the above references and explicitly in Section A6.5.3 of ref 10, the same result for $\Gamma_2 \simeq \Gamma(q)$ (obtained rigorously from the coupled modes) emerges if the ion cloud relaxation is assumed to be much faster than the relaxation of the polymer concentration, within a small numerical prefactor of order unity.

The factor $\kappa_1^2 M_1$ depends on concentration as well as on diffusion constants of counterions and co-ions. We emphasize that screening of hydrodynamic effects is explicitly accounted for in the derivation of eq 11 and the appearance of the solution viscosity (instead of the solvent viscosity) in eq 11 is one indication of this. However, eq 11 is valid for $qR_g < 1$, where R_g is the radius of gyration of the chains, due to the fact that screening of hydrodynamic interactions is also wave-vector dependent like the decay rate, $\Gamma(q)$. We have analyzed an analog of eq 11 valid in the limit $qR_g > 1$ obtained by assuming that hydrodynamics are screened beyond a hydrodynamic screening length, ξ_h, which results in a nonmonotonic dependence of $\Gamma(q)$ on q for the ratio of the correlation length and hydrodynamic length $\xi/\xi_h = 0.79$ predicted for low salt conditions[23] (Figure S10 in the Supporting Information). As no such nonmonotonic dependence of the decay rate is observed in the NSE experiments, we choose eq 11, which is a quasi-one-component description of polyelectrolyte solutions, to analyze the relation between structure and dynamics.

To understand how $\Gamma(q)$ depends on the wavevector as well as polymer and salt concentration, we fit the extracted values of $\Gamma(q)/q^2$ to this theoretical prediction (eq 11). As per the theory,[23] $\Gamma(q) \sim q^0$ for $q\xi \to 0$ and $\Gamma(q) \sim q^3$ for $q\xi > 1$ (see Figure S5). For the experimental data at $q\xi > 2$, we attribute an apparent saturation of $\Gamma(q)/q^2$ to a combination of intermediate dynamics commonly observed in semidilute polymer solutions[14,50,51] as well as limits of instrumental resolution introducing additional error. For fitting purposes, we use solution viscosity η as a fit parameter and the predicted functional form for the static structure factor $S_{pp}(q) \sim q^2/(1 + q^4\xi^4)$, where ξ is obtained by fitting the SANS data in Figure 1. The prefactor in $S_{pp}(q)$ is not required as the ratio of S_{pp} at two different wave-vectors appears in eq 11, and the factor of $\kappa_1^2 M_1$ does not strongly affect the fit values (Figure S9 in the Supporting Information). Fits for salt-free solutions (Figure 2c) and for solutions containing 0.01 and 0.1 M NaCl (Figure S3) capture dependencies of $\Gamma(q)$ on q and on polymer and salt-concentration, with only slight discrepancies, implying that eq 11 along with the predicted form for $S_{pp}(q)$ captures quantitative details of $\Gamma(q)$.

The comparisons presented in Figure 2b,c suggest that the inclusion of hydrodynamic interactions is necessary to capture the wavevector dependence of $\Gamma(q)$. As an additional test, we performed Langevin dynamics simulations of flexible, negatively charged polyelectrolytes with neutralizing counterions[28] (details are provided in Supporting Information; Figures S6 and S7). These simulations lack long-range hydrodynamic interactions but account for topological and electrostatic interactions. We, therefore, expect that a framework without hydrodynamics (i.e., fully screened hydrodynamics) should be able to describe the wavevector dependence of the coupling between the structure and dynamics being simulated in a qualitative manner. Indeed, we observe that the structure and dynamics in the Langevin dynamics simulations are inversely coupled and in good agreement with $\Gamma/q^2 = k_bT\mu/S_{pp}(q)$ (Figure 2d). Specifically, the inverse relationship between structure and dynamics captures both the peak position and the shape around $q\xi = 1$. However, these implicit-solvent simulations predict $\Gamma(q) \sim q^2$ for $q\xi > 1$ (see Figure 2d), which is in disagreement with the experimental results where $\Gamma(q) \sim q^3$ is observed. In our recent work using coarse-grained molecular dynamics simulations with explicit-solvent, we have shown that $\Gamma(q) \sim q^3$ for $q\xi > 1$, which is also expected for Zimm-like relaxation (see Figure 10 in ref 32).

From these simulations, we demonstrate that the coupling between polymer structure and electrostatics results in a nondiffusive dynamic mode and that a full accounting of hydrodynamic effects is required to quantitatively capture the experimental measurements. Together, the results presented in Figure 2 confirm that the effects of hydrodynamic interactions must be taken into account to quantitatively describe the wavevector and salt and polymer concentration dependence of the experimentally measured dynamics.

Equation 11 provides a quantitative prediction of the decay rate. To demonstrate this point, we compare the values of η extracted from the theory to the experimentally measured solution viscosities. The close agreement between the extracted and measured viscosities (Figure 3) confirms that the quasi-one-component description of polyelectrolyte dynamics quantitatively predicts $\Gamma(q)$ for different salt and polymer concentrations. It should be noted, however, that the theory for static structure factor[22] only describes the polyelectrolyte peak and the enhanced scattering at lower wavevectors is not included in the calculations of the decay rate. To determine whether the enhanced scattering at lower wavevectors affects the near-quantitative agreement between the theory and the experiments, we used the measured SANS intensity and the experimentally measured η to calculate $\Gamma(q)$ for all solutions and found only a qualitative agreement with the experimentally measured dynamics (see Figure S4 in the Supporting Information). The origin of this disagreement may lie in the numerical integration of the noisy experimental SANS data,

https://doi.org/10.1021/acs.macromol.3c02564
Macromolecules 2024, 57, 2888−2896

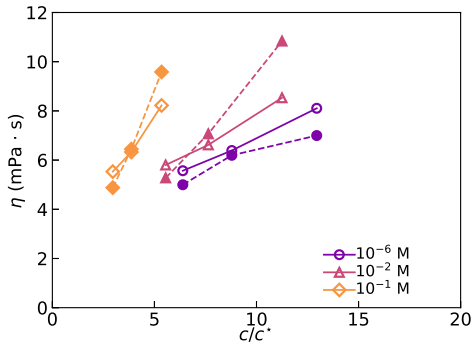

Figure 3. Comparisons of estimated (solid lines) and measured (dashed lines) viscosities (i.e., η) of the polyelectrolyte solutions.

especially at lower wavevectors, but may suggest that the structure at much longer length scales than ξ can affect the decay rate.

Overall, we stress that the combination of the screening effects, which gives rise to the theoretical functional form for the static structure factor $S_{pp}(q)$, and hydrodynamics, which leads to the decay of concentration fluctuations, provides a quantitative description of the polyelectrolyte solutions. We note that eq 11 is an enormous simplification of length scale-dependent dynamics due to the fact that it represents a quasi-one component description accounting for three (i.e., polymer chains, counterions, and solvent) and four (i.e., polymer chains, counterions, co-ions, and solvent) component polyelectrolyte solutions without and with salt, respectively. Despite this simplification, eq 11 is applicable to neutral polymers and small molecules with appropriate modifications (Figure S8 in the Supporting Information) and, in the absence of electrostatics, becomes the Kawasaki[52]−Ferrell[53] formula based on mode decoupling. The Kawasaki-Ferrell mode-decoupling approach has been generalized to multicomponent polyelectrolyte solutions[18−21] using a method developed by Doi and Edwards.[48] These studies, however, used partial static structure factors derived under the assumptions of RPA, which is not applicable for semidilute solutions as confirmed by our SANS results and by others.[40,43,44] Beyond just capturing the nondiffusive relaxations around q^*, this quasi-one component theory also predicts a finite $\Gamma(q)$ even in the limit $q \to 0$, similar to a plasma oscillation[54] and is called a "plasmon mode."[18] In polyelectrolyte solutions, this mode has been predicted to arise from collective displacement of ionic clouds to restore local electroneutrality.[18,55] Our experimental data are consistent with this theoretical prediction of finite $\Gamma(q)$ as $q \to 0$. Direct confirmation of this theoretical prediction would require experiments to currently inaccessible wavevectors and would need to account for the large-scale structures commonly observed in polyelectrolyte solutions. We are aware of only one other recent NSE study on PSS solutions,[56] which did not provide viscosity data and hence was not compatible with the analysis pathway of this study. We anticipate, however, that our study will enable other groups to apply the triple-screening model developed by Muthukumar.

4. CONCLUSIONS

In summary, we have studied the dynamics of concentration fluctuations in semidilute solutions of salt-free and salted NaPSS using neutron scattering, theory, and molecular simulation. The decay rates of the concentration fluctuations measured using NSE depend on the wavevector, polymer, and salt concentration. These dependencies are captured by a quasi-one component description of semidilute polyelectrolyte solutions containing solvent, chains, counterions, and co-ions. In particular, Ferrell's mode decoupling argument[53] and its application to polyelectrolyte solutions by Muthukumar[23] along with double screening[22] of monomer−monomer interactions provide a simple yet quantitatively accurate description of the decay rate.

We expect that our results for aqueous solutions containing NaPSS and NaCl should be readily generalizable to other polyelectrolytes and salts. Thus, this model provides a route to quantitatively understand the dynamics in this biologically important class of materials. Open questions remain about the physics controlling the structure of semidilute polyelectrolyte solutions, particularly at low wavevectors, and its effect on dynamics. Charge regulation-mediated attraction among polyelectrolyte chains has been shown to capture the upturn and the polyelectrolyte peak in concentrated solutions and melts.[13] A similar calculation for semidilute solutions, however, has not been attempted. Additionally, at high wavevectors, the dynamics should follow the Zimm relaxations so that $\Gamma(q) \sim q^3$ for $q\xi > 1$ (cf. Figure S5) and eq 11 captures this limiting behavior. Further, relaxing the condition that counterions and co-ions are at steady state, it can be shown that an additional negative contribution in the total dynamic structure factor arises, corresponding to the fast relaxation of the ionic cloud. These contributions need to be studied separately by analyzing dynamics of counterions and co-ions.[57] Finally, we hope to compare the low wavevector limit of the decay rate obtained from NSE with the diffusion constants measured in DLS experiments.[12,49,58] These developments should lead to a quantitative description of the ionic conductivity of polyelectrolyte solutions relevant to polymer electrolytes, membranes, and biologically relevant phenomena such as translocation of polyelectrolytes.

■ ASSOCIATED CONTENT

Data Availability Statement

The data that support the findings of this study are available from the corresponding author upon reasonable request.

Supporting Information

The Supporting Information is available free of charge at https://pubs.acs.org/doi/10.1021/acs.macromol.3c02564.

Rheology data, and additional SANS data along with details of the implicit-solvent Langevin dynamics simulations and predictions of the triple-screening theory (PDF)

■ AUTHOR INFORMATION

Corresponding Authors

Rajeev Kumar − *Center for Nanophase Materials Sciences, Oak Ridge National Laboratory, Oak Ridge, Tennessee 37831, United States;* orcid.org/0000-0001-9494-3488; Email: kumarr@ornl.gov

Jacinta C. Conrad − *Department of Chemical and Biomolecular Engineering, University of Houston, Houston, Texas 77204, United States;* orcid.org/0000-0001-6084-4772; Email: jcconrad@uh.edu

https://doi.org/10.1021/acs.macromol.3c02564
Macromolecules 2024, 57, 2888−2896

Authors

Ali H. Slim − *Department of Chemical and Biomolecular Engineering, University of Houston, Houston, Texas 77204, United States*

Antonio Faraone − *Center for Neutron Research, National Institute of Standards and Technology, Gaithersburg, Maryland 20899, United States;* orcid.org/0000-0002-3783-5816

Jan-Michael Y. Carrillo − *Center for Nanophase Materials Sciences, Oak Ridge National Laboratory, Oak Ridge, Tennessee 37831, United States;* orcid.org/0000-0001-8774-697X

Ryan Poling-Skutvik − *Department of Chemical Engineering, University of Rhode Island, Kingston, Rhode Island 02881, United States;* orcid.org/0000-0002-1614-1647

Murugappan Muthukumar − *Department of Polymer Science and Engineering, University of Massachusetts, Amherst, Massachusetts 01003, United States;* orcid.org/0000-0001-7872-4883

Amanda B. Marciel − *Department of Chemical and Biomolecular Engineering, Rice University, Houston, Texas 77005, United States;* orcid.org/0000-0001-9403-396X

Complete contact information is available at: https://pubs.acs.org/10.1021/acs.macromol.3c02564

Notes

This manuscript has been authored by UT-Battelle, LLC, under Contract No. DE6AC05-00OR22725 with the U.S. Department of Energy. The U.S. Government is authorized to reproduce and distribute reprints for Government purposes notwithstanding any copyright notation hereon. The Department of Energy will provide public access to these results of federally sponsored research in accordance with the DOE Public Access Plan (http://energy.gov/downloads/doe-publicaccess-plan).

The authors declare no competing financial interest.

■ ACKNOWLEDGMENTS

Theory and simulation works were supported by the Center for Nanophase Materials Sciences, (CNMS), which is a US Department of Energy, Office of Science User Facility at Oak Ridge National Laboratory. R.K. thanks Dr. Vivek Prabhu (NIST) for discussions about neutron spin echo measurements of charged polymers. A.H.S. and J.C.C. were supported by the National Science Foundation (CBET-2004652, CBET-2113769) and the Welch Foundation (E-1869). A.B.M. was supported by the National Science Foundation (CBET-2113767) and the Welch Foundation (C-2003-20190330). M.M. acknowledges financial support from the National Science Foundation (DMR-2309539) and AFOSR (grant no. FA9550-23-1-0584). Access to NSE was provided by the Center for High Resolution Neutron Scattering, a partnership between the National Institute of Standards and Technology and the National Science Foundation under Agreement no. DMR-2010792. This research used resources of the Oak Ridge Leadership Computing Facility at the Oak Ridge National Laboratory, which is supported by the Office of Science of the U.S. Department of Energy under Contract no. DE-AC05-00OR22725.

■ REFERENCES

(1) Kern, W. Über heteropolare Molekülkolloide. I.: Die Polyacrylsäure, ein Modell des Eiweißes 185. Mitteilung über hochpolymere Verbindungen. *Z. Phys. Chem.* **1937**, *181A*, 249−282.

(2) Alfrey, T.; Berg, P. W.; Morawetz, H. The counterion distribution in solutions of rod-shaped polyelectrolytes. *J. Polym. Sci.* **1951**, *7*, 543−547.

(3) De Gennes, P. G.; Pincus, P.; Velasco, R. M.; Brochard, F. Remarks on polyelectrolyte conformation. *J. Phys. (Paris)* **1976**, *37*, 1461−1473.

(4) Barrat, J.; Joanny, F. Theory of polyelectrolyte solutions. *Adv. Chem. Phys.* **1996**, *94*, 1−66.

(5) Morawetz, H. Revisiting some phenomena in polyelectrolyte solutions. *J. Polym. Sci., Part B: Polym. Phys.* **2002**, *40*, 1080−1086.

(6) Holm, C.; Joanny, J. F.; Kremer, K.; Netz, R. R.; Reineker, P.; Seidel, C.; Vilgis, T. A.; Winkler, R. G.. In *Polyelectrolytes with Defined Molecular Architecture II*; Schmidt, M., Ed.; Springer Berlin Heidelberg: Berlin, Heidelberg, 2004; pp 67−111.

(7) Dobrynin, A. V.; Rubinstein, M. Theory of polyelectrolytes in solutions and at surfaces. *Prog. Polym. Sci.* **2005**, *30*, 1049−1118.

(8) Nagasawa, M. *Physical Chemistry of Polyelectrolyte Solutions*; John Wiley & Sons, Inc, 2015.

(9) Muthukumar, M. 50th anniversary perspective: A perspective on polyelectrolyte solutions. *Macromolecules* **2017**, *50*, 9528−9560.

(10) Muthukumar, M. *Physics of Charged Macromolecules*; Cambridge University Press, 2023.

(11) Ermi, B. D.; Amis, E. J. Domain Structures in Low Ionic Strength Polyelectrolyte Solutions. *Macromolecules* **1998**, *31*, 7378−7384.

(12) Muthukumar, M. Ordinary-extraordinary transition in dynamics of solutions of charged macromolecules. *Proc. Natl. Acad. Sci. U.S.A.* **2016**, *113*, 12627−12632.

(13) Kumar, R.; Lokitz, B.; Long, T. E.; Sumpter, B. G. Enhanced scattering induced by electrostatic correlations in concentrated solutions of salt-free dipolar and ionic polymers. *J. Chem. Phys.* **2018**, *149*, 163336.

(14) Slim, A. H.; Shi, W. H.; Safi Samghabadi, F.; Faraone, A.; Marciel, A. B.; Poling-Skutvik, R.; Conrad, J. C. Electrostatic Repulsion Slows Relaxations of Polyelectrolytes in Semidilute Solutions. *ACS Macro Lett.* **2022**, *11*, 854−860.

(15) Akcasu, A. Z.; Benmouna, M.; Hammouda, B. On the dynamics of polyelectrolyte solutions. *J. Chem. Phys.* **1984**, *80*, 2762−2766.

(16) Belloni, L.; Drifford, M. On the effect of small ions in the dynamics of polyelectrolyte solutions. *J. Phys., Lett.* **1985**, *46*, 1183−1189.

(17) Benmouna, M.; Akcasu, A. Z.; Hammouda, B. Addendum to the paper "On the dynamics of polyelectrolyte solutions. *J. Chem. Phys.* **1986**, *85*, 1712−1713.

(18) Ajdari, A.; Leibler, L.; Joanny, J. Cooperative diffusion in weakly charged polyelectrolyte solutions. *J. Chem. Phys.* **1991**, *95*, 4580−4583.

(19) Vilgis, T. A.; Borsali, R. Mean-field theory of concentrated polyelectrolyte solutions: Statics and dynamics. *Phys. Rev. A* **1991**, *43*, 6857−6874.

(20) Perico, A.; Siciliano, A. Dynamics of Polymers in Concentrated Solutions in the Random Phase Approximation: Stiffness Effect. *Macromolecules* **1995**, *28*, 1709−1710.

(21) Siciliano, A.; Perico, A. Dynamics of Concentrated Weakly Charged Polyelectrolyte Solutions. *Macromolecules* **1996**, *29*, 2068−2074.

(22) Muthukumar, M. Double screening in polyelectrolyte solutions: Limiting laws and crossover formulas. *J. Chem. Phys.* **1996**, *105*, 5183−5199.

(23) Muthukumar, M. Dynamics of polyelectrolyte solutions. *J. Chem. Phys.* **1997**, *107*, 2619−2635.

(24) Kumar, R.; Li, W.; Sumpter, B. G.; Muthukumar, M. Understanding the effects of dipolar interactions on the thermodynamics of diblock copolymer melts. *J. Chem. Phys.* **2019**, *151*, 054902.

(25) Stevens, M. J.; Kremer, K. The nature of flexible linear polyelectrolytes in salt free solution: A molecular dynamics study. *J. Chem. Phys.* **1995**, *103*, 1669−1690.
(26) Chang, R.; Yethiraj, A. Brownian dynamics simulations of salt-free polyelectrolyte solutions. *J. Chem. Phys.* **2002**, *116*, 5284−5298.
(27) Liao, Q.; Carrillo, J.-M. Y.; Dobrynin, A. V.; Rubinstein, M. Rouse dynamics of polyelectrolyte solutions: Molecular dynamics study. *Macromolecules* **2007**, *40*, 7671−7679.
(28) Carrillo, J.-M. Y.; Dobrynin, A. V. Polyelectrolytes in salt solutions: Molecular dynamics simulations. *Macromolecules* **2011**, *44*, 5798−5816.
(29) Bollinger, J. A.; Grest, G. S.; Stevens, M. J.; Rubinstein, M. Overlap Concentration in Salt-Free Polyelectrolyte Solutions. *Macromolecules* **2021**, *54*, 10068−10073.
(30) Radhakrishnan, K.; Singh, S. P. Explicit characterization of counterion dynamics around a flexible polyelectrolyte. *Phys. Rev. E* **2022**, *105*, 044501.
(31) Thurston, B. A.; Grest, G. S.; Stevens, M. J. Overlap Concentration of Sodium Polystyrene Sulfonate in Solution. *ACS Macro Lett.* **2022**, *11*, 217−222. PMID: 35574772.
(32) Carrillo, J.-M.; Wang, Y.; Kumar, R.; Sumpter, B. G. Coarse-grained explicit-solvent molecular dynamics simulations of semidilute unentangled polyelectrolyte solutions. *Eur. Phys. J. E* **2023**, *46*, 92.
(33) Dobrynin, A. V.; Colby, R. H.; Rubinstein, M. Scaling theory of polyelectrolyte solutions. *Macromolecules* **1995**, *28*, 1859−1871.
(34) Han, A.; Uppala, V. V. S.; Parisi, D.; George, C.; Dixon, B. J.; Ayala, C. D.; Li, X.; Madsen, L. A.; Colby, R. H. Determining the Molecular Weight of Polyelectrolytes Using the Rouse Scaling Theory for Salt-Free Semidilute Unentangled Solutions. *Macromolecules* **2022**, *55*, 7148−7160.
(35) Hallinan, D. T.; Balsara, N. P. Polymer Electrolytes. *Annu. Rev. Mater. Res.* **2013**, *43*, 503−525.
(36) Bocharova, V.; Sokolov, A. P. Perspectives for Polymer Electrolytes: A View from Fundamentals of Ionic Conductivity. *Macromolecules* **2020**, *53*, 4141−4157.
(37) Kumar, R.; Mahalik, J. P.; Silmore, K. S.; Wojnarowska, Z.; Erwin, A.; Ankner, J. F.; Sokolov, A. P.; Sumpter, B. G.; Bocharova, V. Capacitance of thin films containing polymerized ionic liquids. *Sci. Adv.* **2020**, *6*, No. eaba7952.
(38) Geise, G. M.; Lee, H.-S.; Miller, D. J.; Freeman, B. D.; McGrath, J. E.; Paul, D. R. Water purification by membranes: the role of polymer science. *J. Polym. Sci., Part B: Polym. Phys.* **2010**, *48*, 1685−1718.
(39) Azuah, R.; Kneller, L.; Qiu, Y.; Tregenna-Piggott, P.; Brown, C.; Copley, J.; Dimeo, R. DAVE: A comprehensive software suite for the reduction, visualization, and analysis of low energy neutron spectroscopic data. *J. Res. Natl. Inst. Stand. Technol.* **2009**, *114*, 341.
(40) Muthukumar, M. Electrostatic correlations in polyelectrolyte solutions. *Polym. Sci., Ser. A* **2016**, *58*, 852−863.
(41) Muthukumar, M. Viscosity of polymer solutions. *J. Phys. A: Math. Gen.* **1981**, *14*, 2129−2148.
(42) Muthukumar, M.; Edwards, S. Screening concepts in polymer solution dynamics. *Polymer* **1982**, *23*, 345−348.
(43) Boris, D. C.; Colby, R. H. Rheology of sulfonated polystyrene solutions. *Macromolecules* **1998**, *31*, 5746−5755.
(44) Colby, R. H. Structure and linear viscoelasticity of flexible polymer solutions: comparison of polyelectrolyte and neutral polymer solutions. *Rheol. Acta* **2010**, *49*, 425−442.
(45) De Gennes, P. Liquid dynamics and inelastic scattering of neutrons. *Physica* **1959**, *25*, 825−839.
(46) Hayter, J.; Janninck, G.; Brochard-Wyart, F.; De Gennes, P. Correlations and dynamics of polyelectrolyte solutions. *J. Phys., Lett.* **1980**, *41*, 451−454.
(47) Kanaya, T.; Kaji, K.; Kitamaru, R.; Higgins, J. S.; Farago, B. Dynamics of polyelectrolyte solutions by neutron spin echo: molecular weight dependence. *Macromolecules* **1989**, *22*, 1356−1359.
(48) Doi, M.; Edwards, S. F. *The Theory of Polymer Dynamics; International Series of Monographs on Physics*; Oxford Univ. Press: Oxford, 1986.
(49) Muthukumar, M. Collective dynamics of semidilute polyelectrolyte solutions with salt. *J. Polym. Sci., Part B: Polym. Phys.* **2019**, *57*, 1263−1269.
(50) Poling-Skutvik, R.; Olafson, K. N.; Narayanan, S.; Stingaciu, L.; Faraone, A.; Conrad, J. C.; Krishnamoorti, R. Confined Dynamics of Grafted Polymer Chains in Solutions of Linear Polymer. *Macromolecules* **2017**, *50*, 7372−7379.
(51) Richter, D.; Monkenbusch, M.; Arbe, A.; Colmenero, J. *Neutron Spin Echo in Polymer Systems*; Springer, 2005; pp 1−221.
(52) Kawasaki, K. Kinetic equations and time correlation functions of critical fluctuations. *Ann. Phys.* **1970**, *61*, 1−56.
(53) Ferrell, R. A. Decoupled-Mode Dynamical Scaling Theory of the Binary-Liquid Phase Transition. *Phys. Rev. Lett.* **1970**, *24*, 1169−1172.
(54) Kittel, C. *Introduction to Solid State Physics*, 8th ed.; Wiley, 2004.
(55) Berne, B. J.; Pecora, R. *Dynamic Light Scattering: With Applications to Chemistry, Biology, and Physics*; Wiley: New York, 1976.
(56) Buvalaia, E.; Kruteva, M.; Hoffmann, I.; Radulescu, A.; Förster, S.; Biehl, R. Interchain Hydrodynamic Interaction and Internal Friction of Polyelectrolytes. *ACS Macro Lett.* **2023**, *12*, 1218−1223.
(57) Prabhu, V. M.; Amis, E. J.; Bossev, D. P.; Rosov, N. Counterion associative behavior with flexible polyelectrolytes. *J. Chem. Phys.* **2004**, *121*, 4424−4429.
(58) Jia, D.; Muthukumar, M. Effect of Salt on the Ordinary−Extraordinary Transition in Solutions of Charged Macromolecules. *J. Am. Chem. Soc.* **2019**, *141*, 5886−5896.

https://doi.org/10.1021/acs.macromol.3c02564
Macromolecules 2024, 57, 2888−2896